Development of Novel Wear Equation of AA7050/SiC-Steel Interface for High Temperature Application

Varghese Thaya VIJUMON, Jacob Thambi Evans JEBEEN MOSES *, Poniface JOSE ALOYSIUS, Muthu Nadar FELIX XAVIER MUTHU

Department of Mechanical Engineering, St. Xavier's Catholic College of Engineering Chunkankadai, Nagercoil, Tamil Nadu, India

http://doi.org/10.5755/j02.ms.34486

Received 29 June 2023; accepted 30 August 2023

AA7050 aluminium alloy used for the main landing gear link was reinforced with SiC particles utilizing stir casting and uniform dispersion of reinforced particles was analyzed through SEM with EDS mapping. Wear test were performed on pin on disc apparatus by varying the process parameters and experimental runs were designed using response surface methodology. The influence of SiC particles on wear resistance at high temperatures was explored and the findings led to the development of a novel wear equation. The hardness of composites increased due to impediments of dislocation movement, and it declines with an increase in temperature owing to a reduction of Pierls stresses. The formation of a Mechanically Mixed Layer (MML) enhances wear resistance with the inclusion of reinforced particles, and the breakdown of this layer swifts the wear from moderate to severe. The mode of wear was a combination of shearing and abrasive at room temperature, shearing and adhesive until the temperature 200°C, and plastic deformation when the temperature exceeded 200 °C, which was confirmed by worn surface morphology.

Keywords: tribology, stir casting, scanning electron microscopy, composites, microstructure, high temperature.

1. INTRODUCTION

AA7050 found its application in the main landing gear link because of its superior physical and corrosion properties. However, it displayed deficient tribological behavior, which can be addressed by introducing reinforcing particles [1]. Reinforcing materials include fibres, whiskers, and particles, with Boron Carbide (B_4C), Silicon Carbide (SiC), Aluminium Oxide (Al_2O_3) and graphite being the most common particles utilized to reinforce the aluminium alloy [2, 3]. Due to its enhanced hardness, silicon carbide is an excellent choice for reinforcing and improving the characteristics of lightweight aluminium alloy matrixes [4]. The properties of the aluminum–silicon carbide particle composites vary as the proportion of Sic particles increases and it improves the aluminium matrix's strength, modulus, thermal stability and abrasive wear resistance [5]. The intense proportion of SiC particles as a reinforcing material produces a secondary stage which influence the material properties of composites [6]. Powder metallurgy, casting, in-situ and surface coatings are the distinct composites manufacturing methods of which stir casting was cost effective and potable for mass production [7, 8]. AA7050 and SiC have comparable densities, stir casting is a viable option for making AA7050/SiC composites of distinct weight proportion at a reasonable cost [9].

Lee et al reinforced AA6061 with SiC particles and reported that the wear rate of composites reduces as the size and volume fraction of reinforced particles increases [10]. Garcia-Cordovilla et al reported the same after investigating the wear properties of stir-casted A339/SiC, AA6061/SiC, A357/SiC, and AA6061/Al_2O_3 composites [11]. Numerous efforts have been made to study the impact of process parameters on the wear behavior of composites, by varying load, velocity, sliding distance, temperature, type, size, and proportion of the reinforcement [12]. When the mated sides moved relative to one another, four types of wear predominantly occurred: abrasive, adhesive, fatigue and corrosive/oxidative wear [13]. Abrasive wear was significantly more effective in composites with larger reinforcing particles than in those with smaller ones [14]. This wear rate can be reduced by the formation of the Mechanical Mixed Layer (MML) [15], and but at high temperature this MML breaks down, the wear rate shifts from moderate to severe [16]. Researchers have been working on this problem for the past two decades to find a solution. From the above literature survey, it was evident that, enormous studies have been conducted with regard to the wear investigation of composites fabricated through stir casting, however research related to reinforcing AA7050 alloy with SiC particles was scarcely available. In this work, A wear equation was developed by linking hardness, wear process parameters, weight % of reinforcing particles, and temperature to govern the wear condition which was a novel approach. The worn surface morphology was analyzed using a Scanning Electron Microscope (SEM).

2. EXPERIMENTAL WORK

About 1kg of AA7050 aluminium alloy, as procured from the perfect metal alloys, was placed in the graphite crucible and heated to the temperature of 850 °C using a stir casting furnace. SiC with a particle size of 5 µm was

* Corresponding author. Tel.: +91- 98436 25292;
E-mail: *jebeen@sxcce.edu.in* (J. Jebeen Moses)

purchased from Bhukhanval Industries and preheated to a temperature of 250 °C to remove the moisture content. To improve the wettability of the composites, K_2TiF_6 was added as a flux; the quantity of flux added was equal to the weight proportion of the reinforcing particles. Once the flux was added, the mixture was stirred for 10 min using the 3arm mechanical stirrer at the speed of 750rpm, before being poured into the preheated mould made of die steel. The same procedure was followed for manufacturing composites of distinct weight percentage (0, 2.5, 5, 7.5, 10 wt.%) and the fabricated composites were turned and faced to eliminate the surface defects. The uniform dispersion of composites was analyzed with SEM with EDS mapping (EVO – 18, Carl ZEISS, Germany). The hardness tests were carried out in accordance with ASTM E18-20 standards, with a 100N applied load and a dwell time of 15 s, and the data were recorded on the 'B' scale. Wear experiments were performed on the composites by varying reinforcement weight percentage, temperature, velocity, load and distance as per ASTM G99 standards. Each wear parameter was varied for five levels (levels selected based on trial run), and experimental runs were designed using response surface methodology as depicted in the Table 1, with testing conducted on steel counter face.

Table 1. Wear parameters and their level

S.No	Parameters	Levels
1	Reinforcement, wt.%	0, 2.5, 5, 7.5, 10
2	Temperature, °C	50, 100, 150, 200, 250
3	Load, N	15, 30, 45, 60, 75
4	Velocity, m/s	1.5, 3.0, 4.5, 6.0, 7.5
5	Distance, m	1000, 2000, 3000, 4000, 5000

Each experiment was repeated three times and the average value was taken as the wear rate. The experiments were conducted on Ducom pin on disc tribometer and the wear samples are depicted in Fig. 1.

Fig. 1. Wear samples of AA7050/SiC composites

The worn surface morphology was investigated using a Scanning Electron Microscope (SEM).

3. RESULTS AND DISCUSSION

The microstructure of the composites was depicted in the Fig. 2 which revealed that the reinforced particles were uniformly distributed over the matrix material. Fluoride, found in K_2TiF_6, escaped as white fumes during casting, potassium eliminates impurities and removed as slag, and Ti coats the reinforcing particles and increases the wettability of the composites [17].

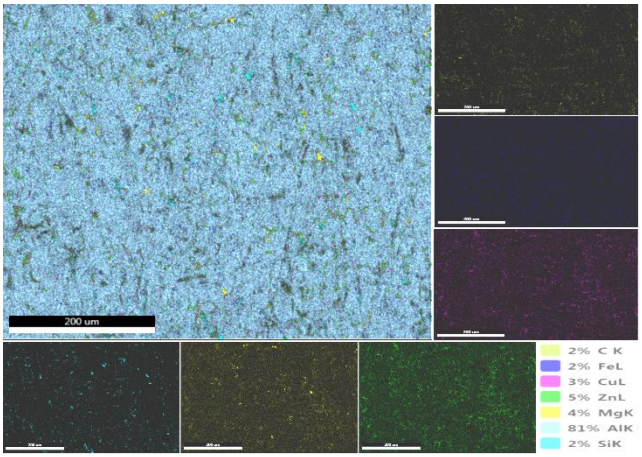

Fig. 2. EDS Mapping of AA7050/SiC composites

The hardness of the composites embellishes with the addition of reinforcing particles as it hampers the kinesis of dislocation as shown in Fig. 3. As a result, the higher the number of SiC particles and the more homogeneous their dispersion, the more hurdles to dislocation movement, hence hardness increases with the addition of particles as reported by distinct researchers [18, 19]. Due to decreased Pierls stresses, increased disorder agility and the eventual initiation of additional slip systems, the hardness of the composites decreases as the temperature rises [20]. From the results, it was revealed that Reinforcement weight percentage (R) was directly proportional and Temperature (T) was inversely proportional to the hardness as depicted in the Eq. 1 and Eq. 2:

$$R \propto H; \tag{1}$$

$$T \propto \frac{1}{H}. \tag{2}$$

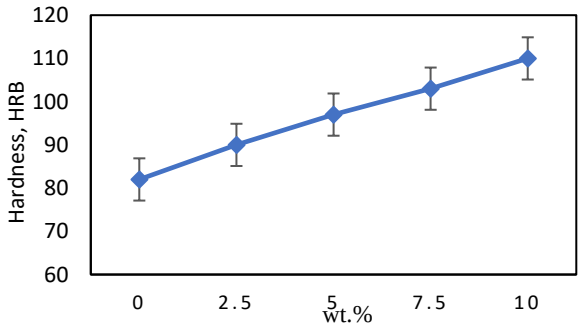

Fig. 3. Hardness of AA7050 composites

The wear rate reduces with rise in the weight percentage of the composites, as it possesses a harder surface following the Archard principal as shown in Fig. 4. The wear rate was the function of applied load (P), sliding velocity (V), sliding distance (L), hardness (H), temperature (T) and it changes over time (t) as portrayed in Eq. 3. Experimental results revealed that the augments in the mentioned functionalities increase the wear rate, an exception was hardness well correlated with the Archard law as depicted in Eq. 4 [21].

$$\frac{\partial W}{\partial t} = f\left\{\frac{\partial P}{\partial t}, \frac{\partial V}{\partial t}, \frac{\partial L}{\partial t}, \frac{\partial H}{\partial t}, \frac{\partial T}{\partial t}\right\}. \tag{3}$$

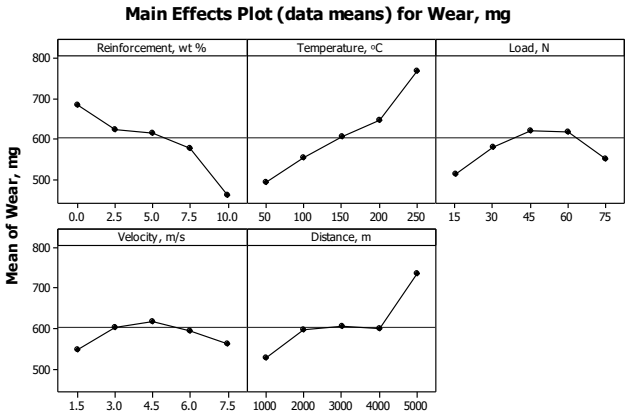

Fig. 4. Impact of various process parameters on wear of AA7050 composites

The surface exerts very high pressure as the load increases, and materials are removed by shearing action, in the case of composites, materials were removed by abrasion and shearing, with abrasion being the dominating contributor [22]. The nominal surface of the contact increases as the load exceeds 45 N, resulting in adhesive wear and a smoother surface, lowering the wear rate. When the sliding temperature is generated between the contact surface, it accelerates shearing and high volume of materials is removed from the surface. When temperature was the function of wear, shearing was the dominant factor, even for the materials reinforced with abrasive particles. When two bodies slide at a velocity exceeding 4.5 m/s, the surface perturbations don't have sufficient time to latch into one other, resulting in a drop in the Coefficient of Friction (CoF) [23]. Because the wear rate was a function of the COF, as the COF lowers owing to higher velocity, the wear rate decreases.

$$W = k.\frac{PLVT}{H}. \tag{4}$$

When the composites slide over the counter disc, the reinforced particles detach from the surface and facilitate the third body abrasion. These particles abrade materials from the counter face and composites pin, forming a Mechanically Mixed Layer (MML) between the surfaces [24], thwarts direct metal-to-metal contact and increasing wear resistance, hence the previous math can be modified as equation 5. Concerning to the sliding distance, the wear rate shifts from mild to severe when exceeds the threshold limit, following Yang's law as depicted in equation 6. The transfer was linked to the breakdown of MML resulted in direct surface contact and eventually increased the wear rate [25, 26].

$$W = k.\frac{PLVT}{HR}; \tag{5}$$

$$W = Ae^{-BL}. \tag{6}$$

The temperature at the surface of the composite pin was the functional factor of load, velocity, *CoF*, thermal conductivity (*T*e) and bulk temperature (Tb) as depicted in Eq. 7 [27]. When the pin was heated externally, the wear rate upsurged with rise in temperature, the mode of wear observed was adhesion. Composites produced with higher reinforcement weight percentage showed lesser wear rate at high temperatures, because it offered enhanced resistance to dislocation and possessed lower thermal conductivity [28]. To correlate the temperature functional factors *CoF*, *T*e and *T*b with the wear rate, Eq. 5 was altered as shown in Eq. 8. The sliding distance required to attain the steady-state wear regime can be written as per Eq. 9. *A* and *B* are experimental constants, contingent on the circumstance of wear face viz abrasive, lubricated, corrosive and high temperature whereas *K* is the wear coefficient that depends on the pin-disc interface [29, 30].

$$T = T_b + \frac{\mu T_e \beta (P^{1/2})V}{2(k^{1/2})}; \tag{7}$$

$$W = \frac{KPLV}{2HR}[2T_b + (P^{1/2})V\mu T_e\beta\left(k^{-1/2}\right)]; \tag{8}$$

$$W = \frac{Ae^{-BL_T}}{2KHR}[2T_b + (P^{1/2})V\mu T_e\beta\left(k^{-1/2}\right)]. \tag{9}$$

4. WORN SURFACE MORPHOLOGY

The worn surface morphology of the composite slides at room temperature showed a large number of scratches and pits as shown in Fig. 5 a.

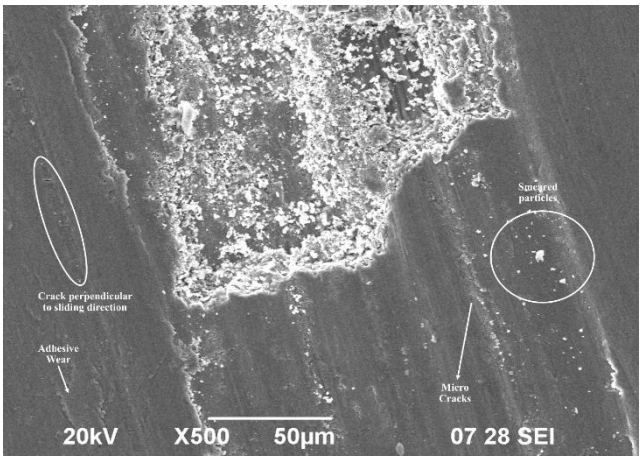

a

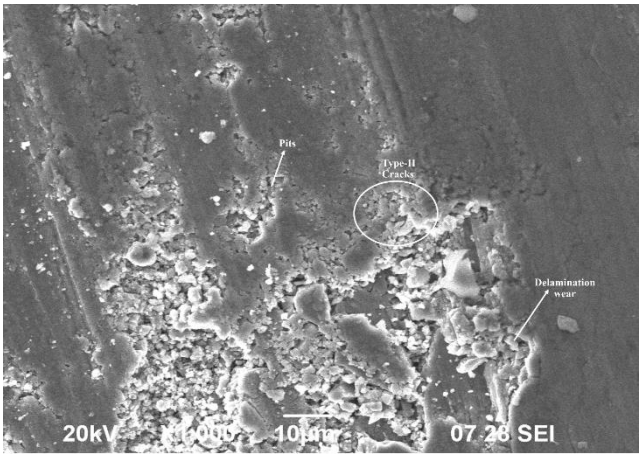

b

Fig. 5. Worn surface morphology of AA7050/SiC composites slides at room temperature (5 wt.%, load 45 N, velocity 4.5 m/s, distance 3000 m): a – at 500X; b – at 1000X

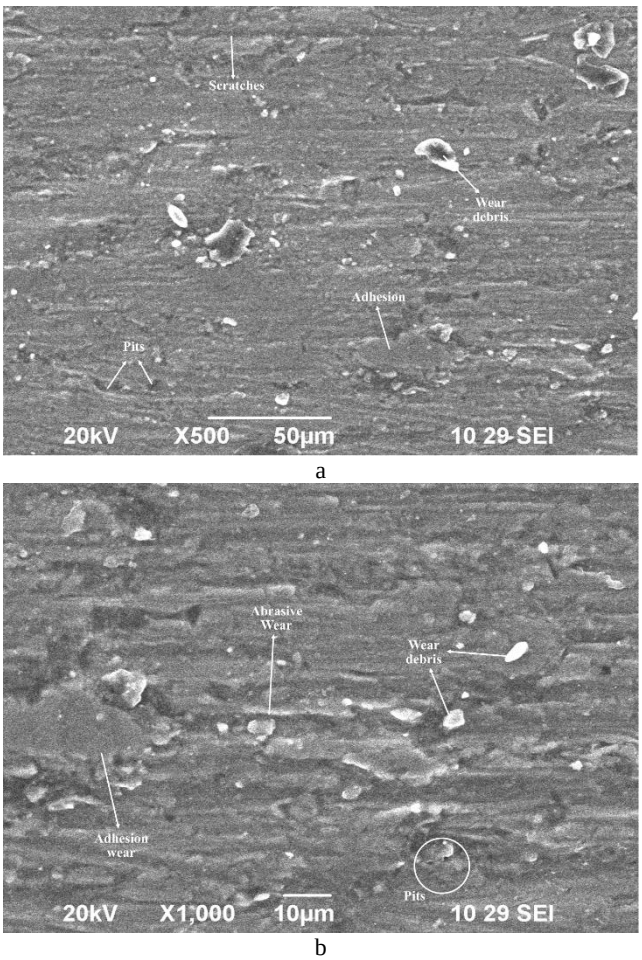

Fig. 6. Worn surface morphology of AA7050/SiC composites slides at 200 °C temperature (7.5 wt.%, load 30 N, velocity 3.0 m/s, distance 4000 m): a – at 500X; b – at 1000X

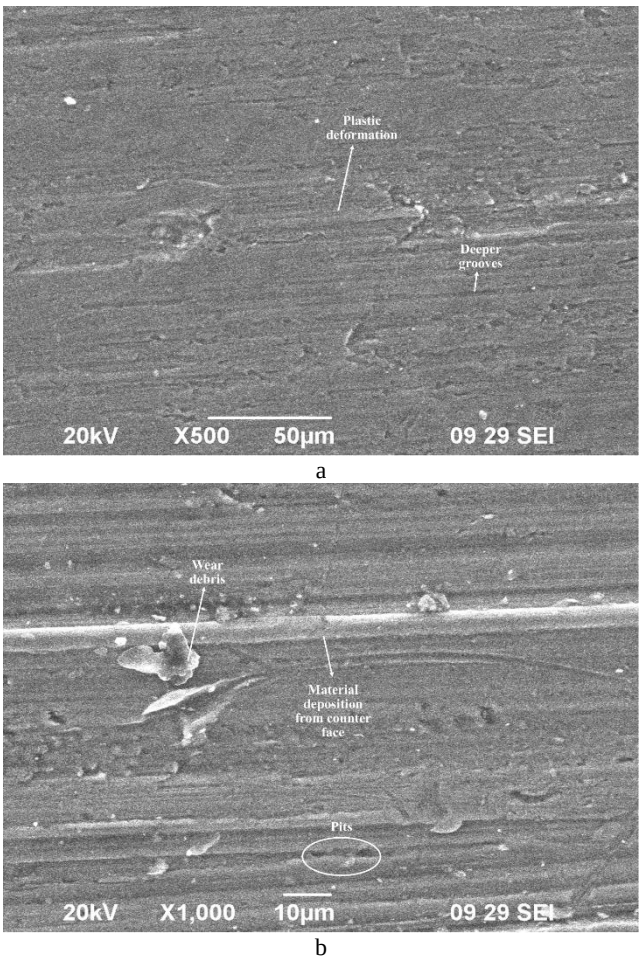

Fig. 7. Worn surface morphology of AA7050/SiC composites slides at 250 °C temperature (5 wt.%, load 45 N, velocity 4.5 m/s, distance 3000 m): a – at 500X; b – at 1000X

The scratches revealed that the reinforced particles detached and reclined in between the surface, scrabbled and triggered the formation of cracks and materials were removed by ploughing. The micrograph revealed that certain fractures occurred perpendicular to the slide direction; in such cases, the materials were removed by shearing, and it also indicated the adhesion mode of wear. At 1000X, the topography showed that the cracks initiated at distinct points and ended in a pit, it combined and ended up in ploughing as shown in Fig. 5 b. The delamination was evident which confirmed that the breakdown of MML occurred well correlated with the investigational verdicts [32]. When slides at the temperature of 200 °C, the confiscated wear debris was stuck back to the surface confirming that the materials attained their recrystallization temperature as shown in Figure 6a. The impression of abrasion marks crafted by the detached reinforced particles were evident but no delamination was noted confirming that shearing and adhesion were the dominant wear mechanism at elevated temperatures. At a higher magnification of 1000X, lumps, deeper groves and pits were visible as shown in Fig. 6 b. A micrograph of an alloy reveals a seized surface, which was distinguished by the creation of lumps along the wear scar.

The surface topography of the specimen slide at 250 °C showed deeper groove and peeling pits as depicted in Fig. 7 a.

The materials were plastically deformed towards the direction of the slide and no hint of ploughing action was observed. The paucity of crack and delamination wear, as well as tiny debris, lumps, and parallel lips, indicated that the mechanism of wear was adhesive. At a higher magnification of 1000X, clumps, structural mounting, thin distortion zone, and narrow mesas indicate a ductile flow as shown in Fig. 7 b. Deposition of the material from the counter face over the pin, irregular shaped debris and pits were observed on the surface. A considerable number of dispersed particles formed along the counter face material deposition zone revealed that material was removed from the counter face due to abrasive wear.

5. CONCLUSIONS

1. The AA7050/SiC was efficaciously manufactured through stir casting technique, SEM with EDS mapping confirmed that the reinforcements were uniformly dispersed over the matrix material.
2. The hardness increases with the weight percentage of the reinforced component due to increased resistance to dislocation movement, and wear resistance increases due to the formation of the MML.
3. A novel wear equation $W = \frac{Ae^{-BL_T}}{2KHR}[2T_b + (P^{1/2})V\mu T_e\beta\left(k^{-1/2}\right)]$ with the function of temperature,

reinforcing weight proportion and wear process parameters was developed and was found to be suitable for predicting the steady-state wear regime of AA7050/SiC/steel interface.

4. Abrasion and adhesion were the dominant wear mechanism at room and elevated temperature, when the temperature exceeds 200°C reinforcing particles have no influence on wear resistance and composites deformed plastically.

6. SCOPE FOR FUTURE WORK

The wear equation was developed for single reinforcement particles; however, the work may be expanded to develop a wear equation for hybrid composites. Work can be expanded further by establishing wear equations for abrasive and lubricated counter faces. The equation can be developed for distinct contact surfaces via teel/magnesium, steel/titanium.

REFERENCES

1. **Prabhakar, N.S., Radhika, N., Raghu, R.** Analysis of Tribological Behavior of Aluminium/B4C Composite Under Dry Sliding Motion *Procedia Engineering* 97 2014: pp. 994 – 1003. https://doi.org/10.1016/j.proeng.2014.12.376
2. **Reddy, P.V., Kumar, G.S., Krishnudu, D.M., Rao, H.R.** Mechanical and Wear Performances of Aluminium-Based Metal Matrix Composites: A Review *Journal of Bio-and Tribo-Corrosion* 6 (3) 2020: pp. 1 – 16. https://doi.org/10.1007/s40735-020-00379-2
3. **Boggarapu, V., Gujjala, R., Ojha, S.** A Critical Review on Erosion Wear Characteristics of Polymer Matrix Composites *Materials Research Express* 7 (2) 2020: pp. 022002. https://doi.org/10.1088/2053-1591/ab6e7b
4. **Faisal, N., Kumar, K.** Mechanical and Tribological Behaviour of Nano Scaled Silicon Carbide Reinforced Aluminium Composites *Journal of Experimental Nanoscience* 13(sup1) 2018: pp. S1 – S13. https://doi.org/10.1080/17458080.2018.1431846
5. **Veerappan, G., Ravichandran, M., Meignanamoorthy, M., Mohanavel, V.** Characterization and Properties of Silicon Carbide Reinforced Ni-10Co-5Cr (Superalloy) Matrix Composite Produced Via Powder Metallurgy Route *Silicon* 13 (4) 2021: pp. 973 – 984.
6. **Bhatia, S., Angra, S., Khan, S.** A Review on Mechanical and Tribological Characterization of Boron Carbide Reinforced Epoxy Composite *Advanced Composite Materials* 30 (4) 2021: pp. 307 – 337. https://doi.org/10.1080/09243046.2020.1759482
7. **Singh, L., Singh, B., Saxena, K.K.** Manufacturing Techniques for Metal Matrix Composites (MMC): An Overview *Advances in Materials and Processing Technologies* 6 (2) 2020: pp. 441 – 457. https://doi.org/10.1080/2374068X.2020.1729603
8. **Balasubramanian, K., Sultan, M.T., Rajeswari, N.** Manufacturing Techniques of Composites for Aerospace Applications *In Sustainable Composites for Aerospace Applications. Woodhead Publishing* 2018: pp. 55 – 67. https://doi.org/10.1016/B978-0-08-102131-6.00004-9
9. **Sanya, O.T., Oji, B., Owoeye, S.S., Egbochie, E.J.** Influence of Particle Size and Particle Loading on Mechanical Properties of Silicon Carbide–Reinforced Epoxy Composites. *The International Journal of Advanced Manufacturing Technology* 103 (9) 2019: pp. 4787 – 4794.
10. **Garcia-Cordovilla, C., Narciso, J., Louis, E.** Abrasive Wear Resistance of Aluminium Alloy/Ceramic Particulate Composites *Wear* 192 (1 – 2) 1996: pp. 170 – 177. https://doi.org/10.1016/0043-1648(95)06801-5
11. **Basavarajappa, S., Chandramohan, G.** Dry Sliding Wear Behavior of Metal Matrix Composites: A Statistical Approach *Journal of Materials Engineering and Performance* 15 (6) 2006: pp. 656 – 660.
12. **Scherge, M., Shakhvorostov, D., Pöhlmann, K.** Fundamental Wear Mechanism of Metals *Wear* 255 (1 – 6) 2003: pp. 395 – 400. https://doi.org/10.1016/S0043-1648(03)00273-4
13. **Padhan, M., Marathe, U., Bijwe, J.** Surface Topography Modification, Film Transfer and Wear Mechanism for Fibre Reinforced Polymer Composites – An Overview *Surface Topography: Metrology and Properties* 8 (4) 2020: pp. 043002. https://doi.org/10.1088/2051-672X/abbcb6
14. **Wang, J., Zhang, G., Chen, N., Zhou, M., Chen, Y.** A Review of Tool Wear Mechanism and Suppression Method In Diamond Turning Of Ferrous Materials *The International Journal of Advanced Manufacturing Technology* 113 (11) 2021: pp. 3027 – 3055.
15. **Du, D., Zhang, W., An, J.** Two Types of Wear Mechanisms Governing Transition Between Mild and Severe Wear In Ti-6Al-4V Alloy During Dry Sliding At Temperatures of 20 – 250°C *Materials* 15 (4) 2022: pp. 1416. https://doi.org/10.3390/ma15041416
16. **Rajamanickam, R., Kumar, S.N.V., Giridharan, P.K., Pradeep, V.** Characterization of Tribological and Mechanical Properties of Aa7050/Al2O3 Composites at Elevated Temperature. High Temperature Material Processes: An International Quarterly of High-Technology Plasma Processes 25 (4) 2021. https://doi.org/10.1615/HighTempMatProc.2021040983
17. **Ranjith, R., Giridharan, P.K., Devaraj, J., Bharath, V.** Influence of Titanium-Coated (B4Cp+ SiCp) Particles on Sulphide Stress Corrosion and Wear Behaviour of AA7050 Hybrid Composites (for MLG Link) *Journal of the Australian Ceramic Society* 53 (2) 2017: pp. 1017 – 1025.
18. **Gürbüz, M., Can Şenel, M., Koç, E.** The Effect of Sintering Time, Temperature, and Graphene Addition on the Hardness and Microstructure of Aluminum Composites *Journal of Composite Materials* 52 (4) 2018: pp. 553 – 563. https://doi.org/10.1177/0021998317740200
19. **Sathish, T., Saravanan, S., Vijayan, V.** Effect of Reinforced Aluminium Alloy LM30 With Pure Ceramic Particles to Evaluate Hardness and Wear Properties *Materials Research Innovations* 2019: pp. 129 – 132. https://doi.org/10.1080/14328917.2019.1614321
20. **Mohanavel, V., Ravichandran, M.** Experimental Investigation on Mechanical Properties of AA7075-AlN Composites *Materials Testing* 61 (6) 2019: pp. 554 – 558. https://doi.org/10.3139/120.111354
21. **Archard, J.F., Hirst, W.** The Wear of Metals Under Unlubricated Conditions *Proceedings of the Royal Society of London. Series A. Mathematical and Physical Sciences* 236 (1206) 1956: pp. 397 – 410. https://doi.org/10.1098/rspa.1956.0144
22. **Akıncıoğlu, G., Uygur, İ., Akıncıoğlu, S., Öktem, H.** Friction-Wear Performance in Environmentally Friendly Brake Composites: A Comparison of Two Different Test

Methods *Polymer Composites* 42 (9) 2021: pp. 4461 – 4477.
https://doi.org/10.1002/pc.26162

23. **Guo, X., Liu, J., Dai, L., Liu, Q., Fang, D., Wei, A., Wang, J.** Friction-Wear Failure Mechanism of Tubing Strings Used in High-Pressure, High-Temperature and High-Yield Gas Wells *Wear* 468 2021: pp. 203576.
https://doi.org/10.1016/j.wear.2020.203576
24. **Du, D., Zhang, W., An, J.** Two Types of Wear Mechanisms Governing Transition Between Mild and Severe Wear in Ti-6Al-4V Alloy During Dry Sliding at Temperatures of 20 – 250°C *Materials* 15 (4) 2022: pp. 1416.
https://doi.org/10.3390/ma15041416
25. **Ranjith, R., Giridharan, P.K., Velmurugan, C., Chinnusamy, C.** Formation of Lubricated Tribo Layer, Grain Boundary Precipitates, and White Spots on Titanium-Coated Graphite–Reinforced Hybrid Composites *Journal of the Australian Ceramic Society* 55 (3) 2019: pp. 645 – 655.
26. **Güney, B.** Corrosion and Wear Behaviour of HVOF Spraying WC-12% Ni Coating on Gray Cast-Iron *Indian Journal of Engineering and Materials Sciences (IJEMS)* 28 (1) 2021: pp. 73 – 81.
http://op.niscpr.res.in/index.php/IJEMS/article/view/34970
27. **Rao, R.N., Das, S.** Wear Coefficient and Reliability of Sliding Wear Test Procedure for High Strength Aluminium Alloy and Composite *Materials & Design* 31 (7) 2010: pp. 3227 – 3233.
https://doi.org/10.1016/j.matdes.2010.02.017
28. **Güney, B., Mutlu, İ.** Wear and Corrosion Resistance of Cr2O3%-40% TiO_2 Coating on Gray Cast-Iron by Plasma Spray Technique *Materials Research Express* 6 (9) 2019: pp. 096577.
https://doi.org/10.1088/2053-1591/ab2fb7
29. **Tabor, D.** Junction Growth in Metallic Friction: The Role Of Combined Stresses And Surface Contamination *Proceedings of the Royal Society of London. Series A. Mathematical and Physical Sciences* 251 (1266) 1959: pp. 378 – 393.
https://doi.org/10.1098/rspa.1959.0114
30. **Elitas, M., Erden, M.A.** Investigation of The Effect of Different Welding Parameters on Tensile Properties and Failure Modes of Non-Alloyed Steel Produced by Powder Metallurgy *Proceedings of the Institution of Mechanical Engineers, Part E: Journal of Process Mechanical Engineering* 2023: pp. 09544089231180542.
https://doi.org/10.1177/09544089231180542
31. **Albahlol, O.A.A., Elkilani, R., Çuğ, H., Erden, M.A., Özmen, R., Esen, I.** Investigation of Microstructure and Mechanical Properties of Layered Material Produced by Adding Al_2O_3 to 316L Stainless Steel *Metals* 13 (7) 2023: pp. 1226.
https://doi.org/10.3390/met13071226